Polymer 50 (2009) 4212–4219

Contents lists available at ScienceDirect

Polymer

journal homepage: www.elsevier.com/locate/polymer

Poly(L-lactide-co-ε-caprolactone) electrospun nanofibers for encapsulating and sustained releasing proteins

Su Yan [a,b,c], Li Xiaoqiang [a,b,c], Tan Lianjiang [a,b], Huang Chen [a,c], Mo Xiumei [a,b,c,*]

[a] State Key Laboratory for Modification of Chemical Fibers and Polymer Materials, Donghua University, Shanghai 201620, China
[b] College of Material Science and Engineering, Donghua University, Shanghai 201620, China
[c] Biomaterials and Tissue Engineering Laboratory, College of Chemistry, Chemical Engineering and Biotechnology, Donghua University, Shanghai 201620, China

ARTICLE INFO

Article history:
Received 19 November 2008
Received in revised form
2 June 2009
Accepted 24 June 2009
Available online 27 June 2009

Keywords:
Coaxial electrospinning
Controlled release
Tissue engineering

ABSTRACT

The aim of this study was to investigate coaxial electrospun poly(L-lactide-co-ε-caprolactone) [PLLACL] nanofibers for the application in nerve tissue engineering. The hypothesis was that the nanofibrous mats fabricated by coaxial electrospun PLLACL could be effective scaffolds for releasing proteins, such as Bovine Serum Albumin (BSA) or/and Nerve Growth Factor (NGF), in a sustained manner. To test the hypothesis, the coaxial electrospun nanofibers with PLLACL as the shell and BSA/NGF as the core were characterized. Morphologies and mechanical properties of nanofibrous mats were examined. BSA released behavior was studied. The results demonstrated that BSA could be sustainedly released from coaxial electrospun PLLACL nanofibers, however, BSA released from mix electrospun nanofibers present the burst release behavior. Bioactivity of released NGF from coaxial electrospun nanofibers was verified by testing the differentiation of rat pheochromocytoma cells (PC12).

1. Introduction

In contrast to conventional transplantation methods, tissue engineering provided new medical therapy which used biomaterials with or without living precursor. The ultimate purpose of tissue engineering is to reestablish the destroyed human tissues or organs by provide scaffolds for functional tissue regeneration. Nerve tissue repair is one of the most serious problems, which directly impacts on the quality of human life [1,2]. One of the effective methods for nerve tissue engineering includes fabrication of polymeric scaffolds with nerve cells to produce a three-dimension tissue and biomaterials functional scaffolds with encapsulation of bioactive proteins (e.g., Nerve Growth Factor) suitable for implantation [3,4]. In human tissue, Extracellular Matrix (ECM) plays a pivotal role in supporting and controlling cells living. For mimicking the human ECM which has a nanofibrous structure, electrospun nanofibers were applied in recent years [5–10]. Nanofibrous scaffolds fabricated by electrospinning of biomaterials provide suitable environment for cell attachment and proliferation, because of the similar physical dimension as natural ECM [11].

Electrospinning technology is a simple and versatile method to prepare ultrathin fibers from polymer solutions or melts [12]. The obtained fibers usually have a diameter from several nanometers to a few micrometers, and mostly in hundreds of nanometers. Electrospun polymer nanofibers possess many extraordinary properties including small diameters and the concomitant large specific surface areas, a high degree of structural perfection and the resultant superior mechanical properties [13]. Additionally, the nonwoven fabrics (mats) made of electrospun polymer nanofibers offer a unique capability to control the pore sizes among nanofibers. Unlike nanorods, nanotubes, and nanowires that are produced mostly by synthetic, bottom-up methods, electrospun nanofibers are produced through a top-down nano-manufacturing process, which results in continuous and low-cost nanofibers that are also relatively easy to be aligned, assembled and processed into applications. Many synthetic and/or natural polymers including, but not limited to, polylactide (PLA) [14], poly(ε-caprolactone) (PCL) [15], poly(glycolic-acid) (PGA) [16], poly(L-lactide-co-caprolactone) (PLLACL) [10], proteins (e.g., collagen), and polysaccharides (e.g., chitosan) [17,18] have been electrospun into nanofibrous mats as tissue engineering scaffolds for growing various kinds of cells. Furthermore, polymer nanofibers obtained through electrospinning have been proposed for using as drug release systems because of outstanding features such as extremely high surface area to volume ratio [19,20]. Electrospun nanofibers have several advantages when compared with other dosage forms; the drug

* Correspondence to: Mo Xiumei, College of Chemistry, Chemical Engineering and Biotechnology, Donghua University, Shanghai 201620, PR China. Tel.: +86 21 67792653.
E-mail address: xmm@dhu.edu.cn (M. Xiumei).

0032-3861/$ – see front matter © 2009 Elsevier Ltd. All rights reserved.
doi:10.1016/j.polymer.2009.06.058

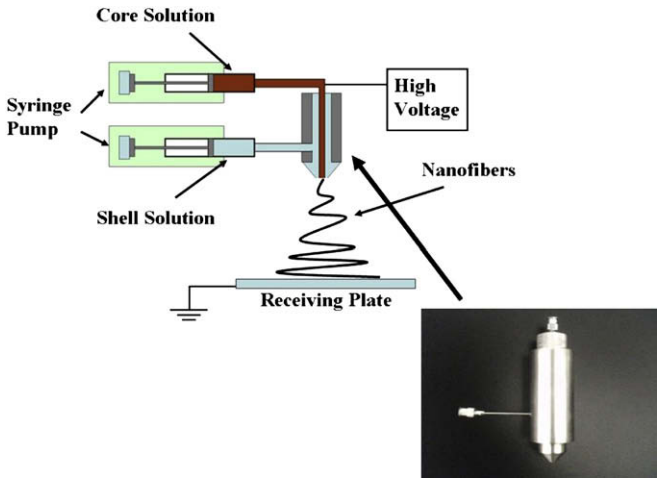

Fig. 1. Basic setup for coaxial electrospinning, the inset picture indicated the special apparatus used in coaxial electrospinning.

release profile can be finely tailored by a modulation on the morphology, porosity, and composition of the nanofibers membrane [21]; the very small diameter of the nanofibers can provide short diffusion passage length; and the high surface area is helpful to a mass transfer and efficient drug release.

Current approaches for nerve tissue repair and nerve regeneration involve encapsulating growth factor or proteins into nanofibers by emulsion and coaxial electrospinning. However, the water-in-oil type emulsion conducted into electrospinning leads to reduce loading efficiency, phase separation and increases protein presence on the surface of fibers rather than uniformly inside the fibers [22]. Recently, many researches have focused on the development of fabricating core–shell type nanofibers by coaxial electrospinning. The core–shell structure nanofibers have many potential applications both in biomedical and tissue engineering fields. These applications included preserving an unstable biological agent from the aggressive environment, preventing the decomposition of a labile compound under a certain condition, delivering a biomolecular drug in a sustained way, and functionalizing the surface of nanostructures without affecting the core material. Sun et al. [23] developed the method of coaxial electrospinning to fabricate core–shell structure for the first time. Several researchers have successfully encapsulated drug into nanofibers by coaxial electrospinning [24–26]. Because proteins is fragile, it is easy to be metamorphosed when mixed with organic molecular which is used as electrospun solvent. However, protein such as Guide Factor is one of the most important biochemical signals for tissue engineering applications. Therefore, how to maintain the bioactivity of proteins during the process of electrospinning has became a stubborn problem for researchers.

In vivo, it has been conformed that when added NGF in the nerve guide tube resulting in an increase in nerve regeneration [4]; based on the study, growth factors from the neurotrophin family has the feasibility to enhance peripheral nerve regeneration. Therefore, nanofibers with NGF incorporating are expected to be used to fabricate nerve guide conduit with the capability of sustain release NGF during the process of nerve self-regeneration.

This study investigated the core–shell structure nanofibrous mats generated by coaxial electrospinning from a PLLACL solution as shell and phosphate buffered saline (PBS, pH 7.4) solution containing proteins as core. PLLACL was selected, because the good properties of attachment and proliferation of both smooth muscle cells (SMCs) and endothelial cells (ECs) had been confirmed in the previous study [10]. Furthermore, the biodegradation rate of PLLALCL could be adjusted by changing the molar ratios of PLLA in the copolymer. The core–shell type nanofibrous mats with bioactive proteins encapsulated in the core were successfully fabricated by coaxial electrospinning. The morphologies of the fabricated nanofibrous mats were examined by scanning electron microscopy (SEM), the mechanical properties both of core–shell type and pure PLLACL nanofibrous mats were measured by a materials testing machine. The release behavior and kinetics of proteins from core–shell nanofibers were measured; the bioactivity of NGF released from nanofibrous mats was confirmed by PC12 neurite outgrowth assay.

2. Materials and methods

2.1. Materials

PLLACL with molar ratio of 50% being L-lactide was purchased from the Sigma–Aldrich Co. (Milwaukee, Wisconsin). 2,2,2-Trifluoroethanol (TFE) was purchased from the Shanghai Fine-Chemicals Co., Ltd. (Shanghai, China). All of the materials were used without further purification.

Recombinant human β-NGF and DuoSet ELISA development system for human β-nerve growth factor were purchased from R&D Systems, Inc. A rat pheochromocytoma cell line, PC12, was obtained from Institute of Biochemistry and Cell Biology of the Chinese Academy of Sciences (Shanghai, China). Phosphate buffered saline (PBS), pH 7.4, containing no calcium chloride and magnesium chloride; and RPMI medium 1640 with L-glutamine were obtained from GIBCO, Invitrogen Corporation. Dichloromethane (99.8% anhydrous) and bovine serum albumin (BSA), fluorescein isothiocyanate conjugate bovine serum albumin (FITC–BSA) were obtained from Sigma–Aldrich Corporation. The serum-free RPMI cell culture medium consists of RPMI 1640 medium, 1% Hepes buffer, 1% sodium pyruvate, 0.275% of penicillin–streptomycin, and 0.556% glucose.

2.2. Electrospinning

The core solution was obtained by adding 0.60 g BSA and 100 μg NGF in 10 mL distilled water, and the shell solution by resolving 0.6 g PLLACL in 10 mL 2,2,2-trifluoroethanol.

The setup equipment briefly consists of a syringe-like apparatus with an inner needle coaxially placed inside an outer one, as shown in Fig. 1. Two syringe pumps (Cole-Parmer Instrument Company, USA) were used to push the solutions from inner and outer needles respectively. The inner needle has an inner diameter of 0.8 mm, and the outer diameter of 10 mm; the outer needle has an inner diameter of 1.8 mm. A copper electrode connected the inner needle directly with high voltage, which means that electrostatic potential was applied to the inner solution only. The electrical potential was transferred to the shell solution through the stainless steel coaxial needles depending on the conductivity of both the core and the shell solutions. An aluminum foil was connected ground to collect ultrafine core–shell structure nanofibers. With an increase in the supplied high voltage to a threshold value, a steady coaxial compound fluid jet was formed and ejected out of the tips of the syringe-like apparatus. The fluid jet was then thinning into submicrometer scale, after evaporation of the solvents during the course of jet flying to the foil; the thin jet was deposited on the collecting screen, forming the coaxial fibers. In our experiment, the inner and outer needle were connected through Teflon tubs to syringe pumps (type YBWZ-12) respectively, using which the core solution was injected at controlled flow rates about 0.05–0.20 mL/h, and the outer one was 1.0 mL/h. The distance between the needles and the collector was set to 10–14 cm. All of the electrospun

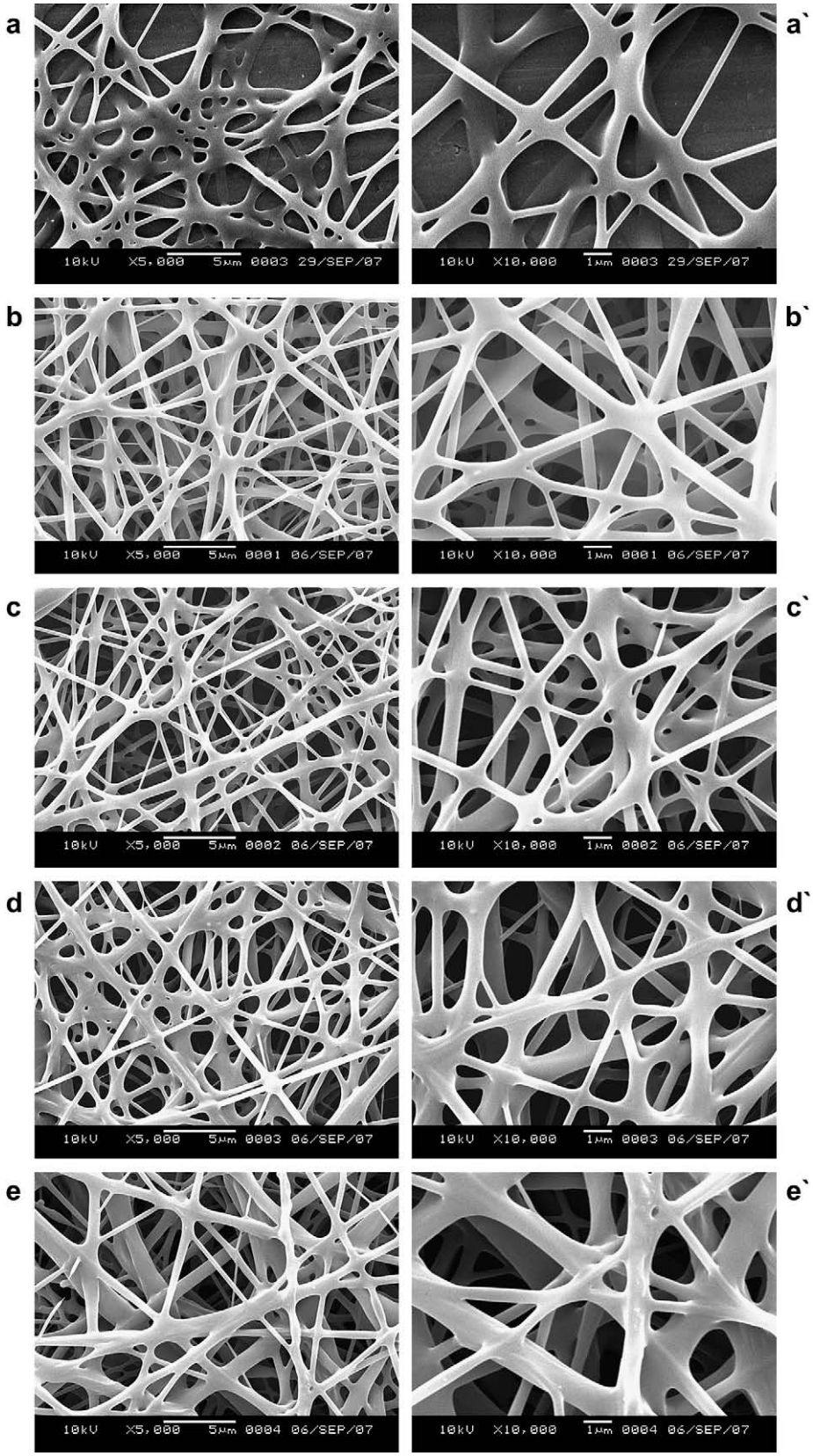

Fig. 2. SEM images of the PLLACL/BSA nanofibers prepared generated from coaxial electrospinning with BSA contents of 5 (a), 10 (b), 15 (c) and 20 (d) wt% compared with PLLACL. (a′), (b′), (c′), and (d′) were the magnification images of (a), (b), (c), and (d) respectively.

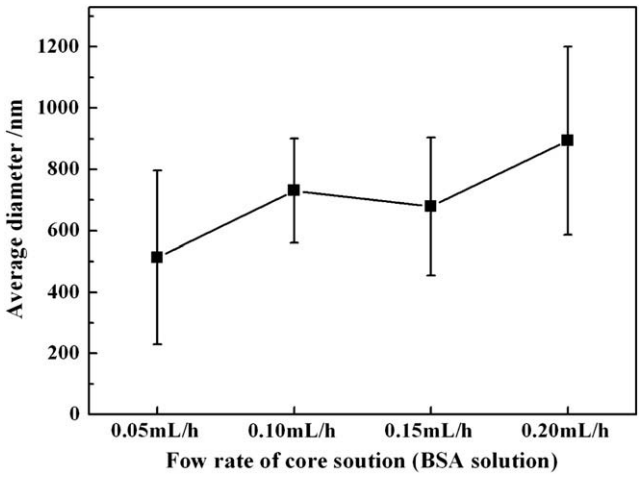

Fig. 3. Average diameters of coaxial electrospun nanofibers from PLLACL and BSA solutions, the flow rates of core solution (BSA solution) were 0.05, 0.10, 0.15, and 0.20 mL/h, respectively.

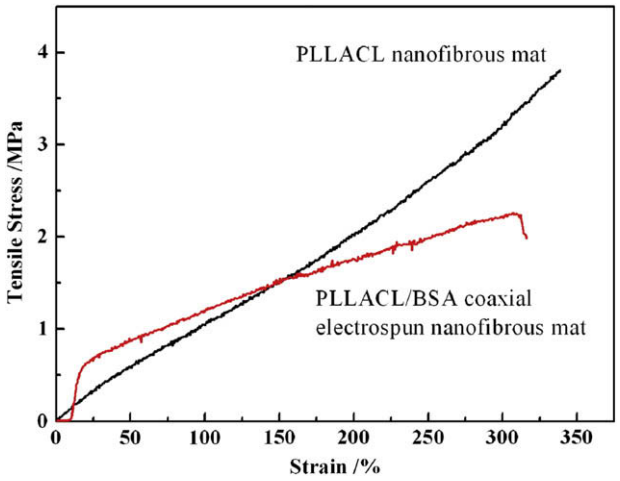

Fig. 4. Representative tensile stress–strain curves of nanofibers mats, the PLLACL nanofibrous mats electrospun from the solution containing 0.06 g/mL PLLACL in TFE, and PLLACL/BSA nanofibrous mats were coaxial electrospun from the 0.06 g/mL PLLACL (as the shell solution, 1.0 mL/h) and 0.06 g/mL BSA in distilled water (as the core solution, 0.10 mL/h).

nanofibers were obtained at ambient temperature of 22–25 °C with a relative humidity of 40–60%.

2.3. Fiber morphology

Morphology of nanofibers was observed by Digital Vacuum Scanning Electron Microscope (JSM-5600LV, Japan Electron Optical Laboratory) at the accelerating voltage of 15 kV. Samples for SEM observations were sputter coated with gold prior to observation. The diameter of the electrospun ultrafine nanofibers was measured with image visualization software Image-J 1.34 (National Institutes of Health, USA). Average fiber diameter and diameter distribution were determined by measuring about 100 random fibers from the SEM images.

2.4. Mechanical property

Mechanical measurements were achieved by applying tensile test loads to specimens prepared from the coaxial electrospun nanofibers mats at the concentration and fluid flow rate mentioned previously. In this study, three specimens were prepared according to the method described by Huang et al. [27]. First, a white paper was cut into templates with width × length = 10 mm × 50 mm and double-side tapes were glued onto the top and bottom areas of one side. And then the aluminum foil was carefully peeled off and single side tapes were applied onto the gripping areas as end-tabs. The resulting specimens had a planar dimension of width × length = 10 mm × 30 mm. Mechanical properties were tested by a materials testing machine (H5K-S, Hounsfield, England) at the temperature of 20 °C and a relative humidity of 65% and a elongation speed of 10 mm/min. Three specimens were tensile tested to calculate the mean values and standard deviations for both pure PLLACL and coaxial electrospun PLLACL/BSA nanofibers mats.

2.5. Encapsulation efficiency of NGF in nanofibers

The loading level and encapsulation efficiency of protein in the PLLACL–BSA nanofibers were determined based on dissolution of PLLACL scaffolds containing BSA in 4 mL 1:1 dichloromethane/PBS solution with 20 mg of scaffolds in triplicate. This would cause the phase transfer where the PLLACL would move to the organic phase and the BSA would move to the aqueous phase. The mixture was vortexed for 1 min followed by centrifugation at 4000 rpm for 5 min. Post-separation, the supernatant (PBS solution containing BSA) was removed and analyzed using UV–vis spectrophotometer. All samples were tested in triplicate. The entrapment efficiency was calculated as the ratio of BSA loaded, estimated from the supernatant, to the total BSA added to the PLLACL–BSA during scaffold fabrication.

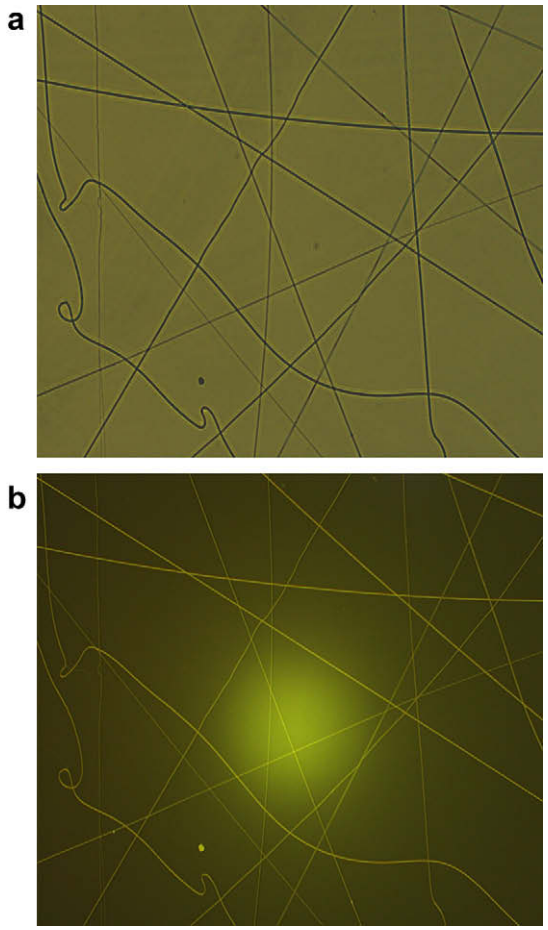

Fig. 5. Distribution of proteins and core–shell structure of BSA/PLACL fibers, (a) optical microscope image of BSA/PLACL fibers on glass slide, (b) fluorescence microscopy image of FITC–BSA/PLACL fibers.

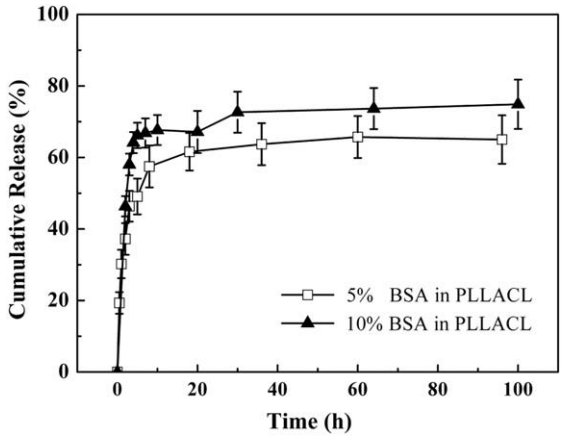

Fig. 6. *In vitro* BSA release profiles from PLLACL nanofibers which were fabricated by mix electrospinning with different BSA proportions.

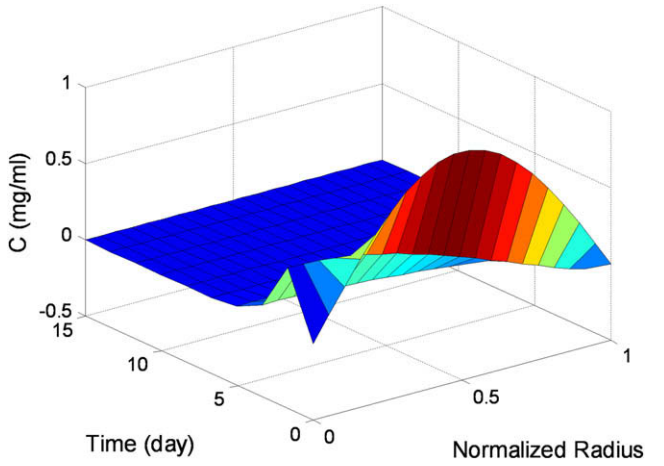

Fig. 8. The relationship between BSA concentration and release time at the direction of fibers radial.

2.6. Protein distribution observation

Protein distribution in the PLACL fibers was evaluated by observing the distribution of FITC–BSA encapsulated in the result fibers by an optical microscope (UL100HG Olympus Corporation, Japan).

2.7. In vitro protein release study

PLLACL nanofibrous mats loaded with different weight ratios of BSA were suspended in PBS (pH 7.4) solution in sealed 12-well plates. Three samples that were electrospun using the same electrospinning parameters were used in this study. The three electrospun fibrous meshes, each weighing 100 ± 5 mg, were each soaked in 3.0 mL of PBS (pH 7.4). Fibrous mats were incubated under static conditions at 37 °C in the presence of 5% carbon dioxide. At various time points, 1.5 mL of supernatant was retrieved from the wells and an equal volume of fresh medium was replaced. And then the concentration of each retrieved BSA solution was determined by measuring the absorbance at 280 nm using a UV–vis spectrophotometer (WFZ UV-2102 Unique Technology Shanghai) in duplicates. It is noted that there was no NGF encapsulated in nanofibers.

As compare, mix electrospinning of PLLACL-blend-BSA were conducted. The mix electrospinning solutions were simply dissolved polymer and BSA in TFE, and then electrospun into nanofibers at the PLLACL concentration of 0.06 g/mL. During mix electrospinning, the mass flows were maintained 1.0 mL/h, and a positive high voltage of 20 kV was applied at the tip of syringe needle with the inner diameter of 0.9 mm.

2.8. In vitro bioactivity study

NGF, stabilized by BSA, was dissolved into 1.0 mL PBS (pH 7.4) solution. The concentrations of NGF/PBS solution were determined by DuoSet ELISA development system. Images of the PC12 cells were taken 48 h after the NGF solutions were added into the culture medium.

The released NGF bioactivity was verified by the method of Chew et al. [4]. PC12 cells were cultured in collagen type IV-coated 24-well plates at a density of 1×10^4 cells/cm^2. A volume of 400 μL of the NGF supernatant from the PLLACL nanofibers was added to each well of PC12 cells and serum-free RPMI was added to top up the medium volume to 1.0 mL per well. As a positive control, 8 μL of 50 μg/mL of NGF solution was added to the PC12 cell culture medium, and the total volume of medium was then topped up to 1.0 mL with serum-free RPMI. A negative control in which no NGF was added to the serum-free RPMI medium was also used. Images

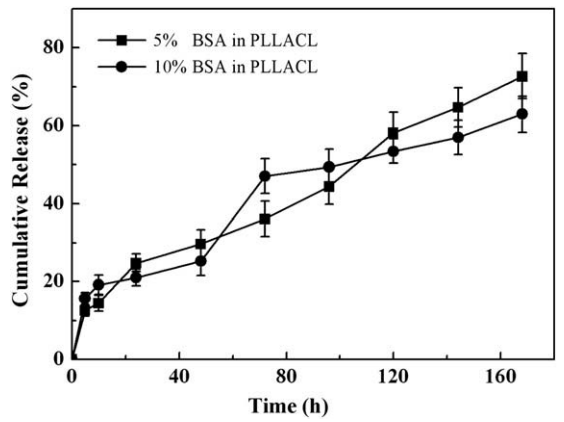

Fig. 7. *In vitro* BSA release profiles from PLLACL nanofibers which were fabricated by axial electrospinning with different BSA proportions.

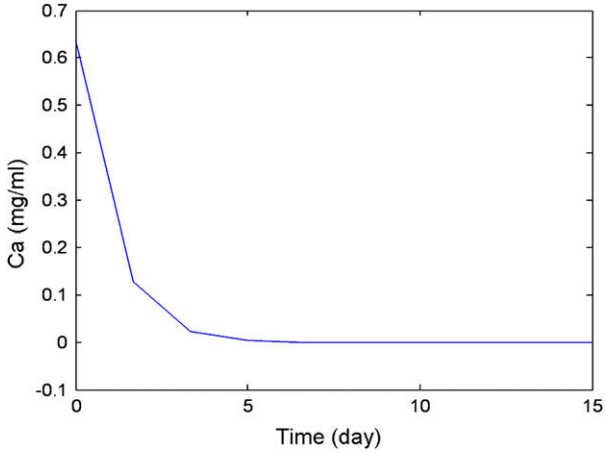

Fig. 9. The relationship between average concentration of BSA in nanofibers and release time.

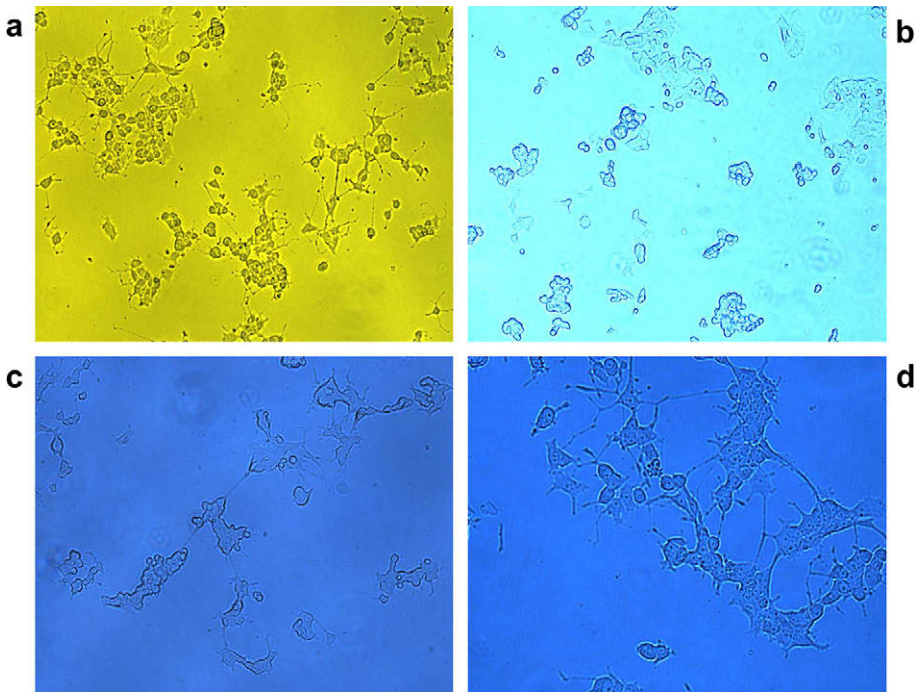

Fig. 10. (a) Positive control of PC12 cells in soluble NGF, (b) negative control of PC12 cells in plain serum-free RPMI medium, (c) PC12 cells in day 1 supernatant, 200×, and (d) PC12 cells in day 10 supernatant, 400×.

of the PC12 cells were taken 48 h after the supernatant was added into the culture medium.

3. Results and discussion

3.1. Fiber morphology and structure

In electrospinning, the polymer solution jet solidifies when it travels from the electrospinning needle to the receiving plate with the evaporation of solvent (s) and the solidified jet turns into a nanofiber. The solvent evaporation during electrospinning occurs only when the following conditions are satisfied: (1) the jet has micron- or submicron-scaled diameter; (2) the jet carries excess charges, which are beyond the surface tension of electrospun polymer solution; (3) the solvent(s) evaporate under the influence of a strong electric field [13]. These result in the abnormally fast evaporation rate of solvents during electrospinning. PLLACL is easy to dissolve in many solvents, such as acetone, chloroform, and 1,1,1,3,3,3-hexafluoro-2-propanol. In this work, a water-solubility solvent TFE was used to prepare PLLACL solution. The effect of polymer concentration on fiber morphology was studied in previous experiments where the polymer concentration ranged from 0.02 g/mL to 0.08 g/mL. The results demonstrated that ultrafine PLLACL nanofibers with smooth surface could be electrospun at the concentrations between 0.04 g/mL and 0.12 g/mL. Different surface morphologies of the nanofibrous mats were observed for PLLACL solutions in TFE with varied concentrations. Furthermore, the fiber diameters increased with the increasing of polymer concentration. In this study, the concentration of polymer solution for coaxial electrospun was chosen at 0.06 g/mL.

The presence of distilled water in core solution could affect the formation of electrospun nanofibers and thus the morphologies of the electrospun nanofibrous mat, because the volatility of solvents is one of the most important influence factors in the solidification of electrospun nanofibers. In our previous study, we found that the higher the water content was, the less uniform the nanofibers in the mat would be, and the higher the water content in the emulsion was, the more likely the nanofibers would conglutinate together in the mats. That is because water has relatively low volatility, and may not be able to completely evaporate during electrospinning. However, as shown by the entire representative images in Fig. 2, nanofibers formed at different flow rates of BSA solutions have similar morphology. It is noted that the flow rates of core solutions (BSA/distilled solutions, 0.05, 0.10, 0.15 and 0.20 mL/h) were very slow compared with the shell rate (1.0 mL/h). Therefore, the influence of water content on the fibers morphology was very small.

Fig. 3 shows the average diameters of coaxial electrospun nanofibers from PLLACL and BSA solutions at different core solution flow rates. Only the non-conglutinated part of fibers was chosen to measure their diameters. The average diameters of coaxial electrospun nanofibers ranged from 500 nm to 840 nm, but there is no proportional relationship between the average diameters of the fibers and the flow rates of core solution. It is also found that the diameter distribution is not uniform as shown in Fig. 2. Some special thin fibers and thick fibers appear in the SEM micrographs. This may be explained by the fact that the main fluid jet from the needle tip split into several sub-jets during the weeping process.

3.2. Mechanical property of coaxial electrospun nanofibrous mats

Coaxial electrospun nanofibers created from PLLACL and NGF were expected to fabricate nerve growth conduit (NGC) for the application of rehabilitating nerve rupture caused by traffic accident or mechanical force. Therefore, mechanical properties of nanofibers are important for the successful application in tissue engineering. In this study, the nanofibrous mats from electrospinning of PLLACL–TFE solution single and coaxial electrospinning (with PLLACL–TFE as the shell solution, 1.0 mL/h, and BSA–distilled

water as the core solution, 0.10 mL/h). The representative tensile stress–strain curves of the electrospun nanofibrous mats are shown in Fig. 4. All of the mats were stretched till break. The average strength of PLLACL nanofibrous mat (black curve in the figure) was 3.47 ± 0.31 MPa, which was higher than that of the coaxial electrospun nanofibrous mat (red curve[1] in the figure, the average ultimate stress of three samples was 2.05 ± 0.14 MPa). This could be attributed to the "core–shell" structure of PLLACL nanofibers, for the BSA in core contributed much less to the mechanical performance. It should be noted that BSA was one kind of protein with low molecular weight, and BSA solution with low concentration couldn't be used to fabricate nanofibers by electrospinning. Nonetheless, the matrix of the coaxial electrospun nanofibrous mat was PLLACL which was identical to that in the neat PLLACL nanofibrous mat; so that the ultimate strain of both nanofiber mats were similar. It is noted that the mechanical properties of nanofibrous mats usually could not be directly translated into the mechanical properties of nanofibers.

3.3. Proteins distribution in nanofibers

As the SEM images cannot provide evidences that proteins were successfully incorporated into polymer fibers, FITC–BSA was conducted for the study of protein distribution in nanofibers. FITC–BSA was used as part of carried materials as well as BSA, and the composite fibers of FITC–BSA/BSA/PLACL were observed by Fluorescence Microscopy (FM, IX71-A12FL, OLYMPUS, Japan). The low amount of FITC–BSA in the electrospun solution had no significant impact on the electrospinning process, allowing the use of the same electrospinning parameters in the formation of BSA-encapsulated fiber. Fig. 5 indicates the distribution of proteins in PLACL fibers. FITC–BSA/PLACL fibers were collected on a glass slide, and then observed by Optical Microscopy (OM) and FM at the same collected point. As shown in Fig. 5b, the fibers emitted fluorescence light, suggesting the presence of FITC–BSA. The appearances of the fibers in Fig. 5a and b are similar. These results confirmed that the proteins were distributed all through PLACL fibers. Because the electrospun parameters of fabricating FITC–BSA/PLACL were the same as fabricating the NGF–BSA/PLACL nanofibers, the distribution of FITC–BSA can be used to represent the NGF–BSA distribution in the PLACL nanofibers.

3.4. In vitro protein release study

BSA release profiles from mix electrospun PLLACL nanofibers with different BSA proportions are shown in Fig. 6. Experiments were performed in triplicate and error bars indicated on standard deviation. The release kinetics for mix electrospinning cases can be illustrated by two stages: an initial fast release before the inflections (stage I) followed by a constant release (stage II). In stage I, there were initial burst releases from mix electrospun mats. Then the release was ceased and the total released amount was 60–80% in stage II. Xu et al. [22] had reported a water-soluble drug capsulated in an oily phase of chloroform solution of amphiphilic poly(ethylene glycol)-poly(L-lactic acid) (PEG–PLLA) diblock copolymer, and they found that the drug release behavior was related with the distribution of drug in the fiber mats. In the process of electrospinning, the irons were easily attracted at the surface of nanofibers, namely, BSA molecules were easily distributed on the surface of nanofibers. During the release processes, BSA presented on the surface was dissolved in PBS solution. Thereafter, the inner presented BSA diffused in PBS in the later phases, but the quantity was very tiny. The encapsulation efficiencies of BSA in PLLACL scaffolds electrospun from blend solution of PLLACL–BSA were found to be $78.5 \pm 4.6\%$ for 5% BSA loaded and $80.2 \pm 5.1\%$ for 10% BSA loaded.

However, the mats derived from coaxial electrospinning showed a relatively stable release behavior of BSA in Fig. 7. The method of coaxial electrospinning made the BSA encapsulated in the inner part of nanofibers during the processes of electrospinning. Some of the BSA also emigrated to the surface of PLLACL nanofibers, because the inner and outer BSA solution solutions could mix together completely. There were also initial stages in the curves of coaxial electrospun PLLACL/BSA nanofibrous mats. But they were quite different from those with the method of mix electrospinning. The profile of BSA released from coaxial electrospun nanofibrous mat present an initial stages of 10–20%, and after these sections, the release curves exhibited sustained behavior. The whole process of release lasted for 108 h till the total released amount was about 70%. It was obvious that the release was not complete, and the rest of the BSA may continue to release for longer time. In this case, the capsulation efficiency of BSA from coaxial electrospinning increased to $93.2 \pm 5.4\%$ for 5% BSA loaded and $89.7 \pm 5.9\%$ for 10% BSA loaded.

3.5. Release kinetics

The mechanism responsible for the relatively steady release of the protein from nanofibers after the burst is unclear. The observation suggests that the diffusion is the predominant mechanism. In an attempt to analyze the diffusion mechanism in more detail, the fibrous mats system was modeled as a cylinder as shown in Fig. 1. The experimental details can only provide the relationship between release amount and time, but not the BSA distribution in nanofibers. Therefore, we developed a model with the aid of MATLAB 7.0 to evaluate the concentration distribution of BSA in PLLACL nanofibrous mats on the basis of diffusion mechanism.

When a cylindrical coordinate is used, the Second Fick's Law can be expressed as:

$$\frac{\partial c}{\partial t} = \frac{1}{r} \cdot \left[\frac{\partial}{\partial r} \left(r \cdot D \cdot \frac{\partial c}{\partial x} \right) \right] \tag{1}$$

In Equation (1):

r – the radial distance;
t – the diffusion time;
D – the diffusion coefficient;
C – the concentration of BSA in nanofibers.

The concentration of BSA was a function of both radial distance and diffusion time. Therefore, initial and boundary conditions are needed to solve this partial differential equation (PDE).

Initial condition (IC): $C = C_0$ ($t = 0$, $0 \le r \le R$). C_0 is the initial BSA concentration in nanofibers.

Boundary condition (BC): $C = C_1$ ($r = R$, $t \ge 0$). C_1 is the BSA concentration on the surface of nanofibers.

$(\partial c/\partial r) = 0$, when $r = 0$, $t \ge 0$.

The standard format of PDE equation in MATLAB is as follows:

$$c\left(x, t, u, \frac{\partial u}{\partial x}\right) \cdot \frac{\partial u}{\partial t} = x^{-m} \cdot \frac{\partial}{\partial x} \left(x^m \cdot f\left(x, t, u, \frac{\partial u}{\partial x}\right) \right) + s\left(x, t, u, \frac{\partial u}{\partial x}\right) \tag{2}$$

m equals 2 in the case of cylindrical coordinate.

The average concentration of BSA in nanofibers was calculated using the following relation:

[1] For interpretation of the references to colour in this text, the reader is referred to the web version of this article.

$$C\_\text{average} = \frac{\sum_{i=1}^{N} \int_{(i-1)R/N}^{iR/N} 2\pi r \, dr \times C_i^a}{\int_0^R 2\pi r \, dr} \quad (3)$$

where $C_i^a = (C_{i-1} + C_i)/2$.

In this study, the relationship between the BSA concentration and the release time had been investigated. The diffusion coefficient D was arbitrarily set as 2×10^{-10} m^2/d, which would not influence the analysis. The initial concentration of BSA in nanofibers was set as $C_0 = 0.60$ mg/mL (the hypothesis is that the concentration of BSA in nanofibers was the same). The concentration of BSA on the surface and out of the nanofibers was 0.00 mg/mL.

The results of calculation using MATLAB are shown in Figs. 8 and 9. In Fig. 8, the BSA concentration along the fiber radius during the release process is depicted via the three-dimensional curved surface. In Fig. 9, at the above conditions, the average concentration of BSA decreased sharply during the first 5 days of release. There was only 1–2% BSA released from nanofibers for the following 10 days. This can also be observed from Fig. 8. The calculated results agreed with the experimental details.

3.6. In vitro bioactivity study

The bioactivity of NGF released from coaxial electrospun nanofibers was analyzed by observing the differentiation of PC12 cells into neurons, in the presence of the supernatant obtained from the electrospun NGF encapsulated fibers. The differentiation of the PC12 cells into neurons in the supernatant and in the controls is shown in Fig. 10. Since the threshold for induction of PC12 cell differentiation is around 0.5 ng/mL, this amount was enough to stimulate up to 15% of the PC12 cells [4]. Culture-to-culture variability is typical in such cellular assays. Positive control was using fresh NGF at a concentration of 200 ng/mL, which had led PC12 cells to differentiate into neurite. The study of adding supernatant which was abstained from NGF released solution at the 10th day into PC12 cells culture medium showed a positive result. This experiment did indicate that the NGF released from the PLLACL fibers retained at least some degree of bioactivity for up to 10 days.

4. Conclusions

In this study we investigated the coaxial electrospun PLLACL nanofibrous as well as explored whether the PLLACL/NGF nanofibrous mat could be utilized as a scaffold for protein delivery system. The coaxial electrospun nanofibrous mats from PLLACL possessed unique combined characteristics of both cell-growth scaffolds and controllable drug releasing agents. PLLACL/NGF nanofibers were successfully prepared by coaxial electrospinning PLLACL solution (as the shell solution) and NGF solution (in combination with BSA, as the core solution). The study of BSA release confirmed that proteins encapsulated in coaxial electrospun nanofibers could be released in a stable and sustained manner. The bioactivity of NGF released from PLLACL nanofibers was investigated using the test of PC12 cells differentiation.

Acknowledgment

This research was supported by National Science Foundation (30570503), National High Technology Research and Developed Program (863 Program, 2008AA03Z305), Science and Technology Commission of Shanghai Municipality Program (08520704600, and 0852nm03400).

References

[1] Chew SY, Mi RF, Hoke A, Leong KW. Adv Funct Mater 2007;17(8):1288–96.
[2] Wang W, Itoh S, Matsuda A, Aizawa T, Demura M, Ichinose S, et al. J Biomed Mater Res A 2008;85A(4):919–28.
[3] Yang F, Murugan R, Ramakrishna S, Wang X, Ma YX, Wang S. Biomaterials 2004;25(10):1891–900.
[4] Chew SY, Wen J, Yim EKF, Leong KW. Biomacromolecules 2005;6:2017–24.
[5] Andrews KD, Hunt JA, Black RA. Polym Int 2008;57:203–10.
[6] Ashammakhi N, Ndreu A, Piras A, Nikkola L, Sindelar T, Ylikauppila H, et al. J Nanosci Nanotechnol 2006;6(9–10):2693–711.
[7] Badami AS, Kreke MR, Thompson MS, Riffle JS, Goldstein AS. Biomaterials 2006;27(4):596–606.
[8] Bhattarai N, Edmondson D, Veiseh O, Matsen FA, Zhang MQ. Biomaterials 2005;26(31):6176–84.
[9] Bashur CA, Dahlgren LA, Goldstein AS. Biomaterials 2006;27(33):5681–8.
[10] Mo XM, Xu CY, Kotaki M, Ramakrishna S. Biomaterials 2004;25(10):1883–90.
[11] Chen ZG, Mo XM, He CL, Wang HS. Carbohydr Polym 2008;72(3):410–8.
[12] Rutledge GC, Fridrikh SV. Adv Drug Deliv Rev 2007;59:1384–91.
[13] Liao YL, Zhang LF, Gao Y, Zhu ZT, Fong H. Polymer 2008;49(24):5294–9.
[14] Corey JM, Gertz CC, Wang B-S, Birrell LK, Johnson SL, Martin DC, et al. Acta Biomater 2008;4(4):863–75.
[15] Bolgen N, Vargel I, Korkusuz P, Menceloglu YZ, Piskin E. J Biomed Mater Res Part B Appl Biomater 2007;81B(2):530–43.
[16] Boland ED, Telemeco TA, Simpson DG, Wnek GE, Bowlin GL. J Biomed Mater Res B 2004;71B(1):144–52.
[17] Chen JP, Chang GY, Chen JK. Colloids Surf A 2008;313:183–8.
[18] Chen ZG, Mo XM, Qing FL. Mater Lett 2007;61(16):3490–4.
[19] Huang ZM, Zhang YZ, Kotaki M, Ramakrishna S. Compos Sci Technol 2003;63(15):2223–53.
[20] Li D, Xia YN. Adv Mater 2004;16(14):1151–70.
[21] Kim K, Luu YK, Chang C, Fang DF, Hsiao BS, Chu B, et al. J Control Release 2004;98(1):47–56.
[22] Xu XL, Yang LX, Xu XY, Wang X, Chen XS, Liang QZ, et al. J Control Release 2005;108(1):33–42.
[23] Sun ZC, Zussman E, Yarin AL, Wendorff JH, Greiner A. Adv Mater 2003;15(22):1929–32.
[24] Zhang CX, Yuan XY, Wu LL, Sheng J. Proceedings of 2005 international conference on advanced fibers and polymer materials (ICAFPM 2005), vols. 1 and 2; 2005. p. 330–3.
[25] Li XQ, Su Y, Chen R, He CL, Wang HS, Mo XM. J Appl Polym Sci 2009;111(5):1564–70.
[26] Cui W, Li X, Zhu X, Yu G, Zhou S, Weng J. Biomacromolecules 2006;7(5):1623–9.
[27] Huang ZM, Zhang YZ, Ramakrishna S, Lim CT. Polymer 2004;45(15):5361–8.